Hindawi Publishing Corporation
International Journal of Oceanography
Volume 2010, Article ID 819029, 11 pages
doi:10.1155/2010/819029

Research Article

Nitrogen Uptake in the Northeastern Arabian Sea during Winter Cooling

S. Kumar,[1,2] R. Ramesh,[1] R. M. Dwivedi,[3] M. Raman,[3] M. S. Sheshshayee,[4] and W. D'Souza[5,6]

[1] *Physical Research Laboratory, Geosciences Division, Navrangpura, Ahmedabad 380 009, India*
[2] *Faculty of Natural Resources Management, Lakehead University, Thunder Bay, ON, Canada P7B 5E1*
[3] *Marine and Water Resources Division, Space Applications Centre, Ahmedabad 380 015, India*
[4] *Department of Crop Physiology, University of Agricultural Sciences, Bangalore 560 065, India*
[5] *Chemical Oceanography Division, National Institute of Oceanography, Goa 403 004, India*
[6] *Department of Chemistry, Goa University, Goa 403 206, India*

Correspondence should be addressed to S. Kumar, skumar2@lakeheadu.ca

Received 1 October 2009; Accepted 5 April 2010

Academic Editor: Walker Smith

The uptake of dissolved inorganic nitrogen by phytoplankton is an important aspect of the nitrogen cycle of oceans. Here, we present nitrate (NO_3^-) and ammonium (NH_4^+) uptake rates in the northeastern Arabian Sea using ^{15}N tracer technique. In this relatively underexplored region, productivity is high during winter due to supply of nutrients by convective mixing caused by the cooling of the surface by the northeast monsoon winds. Studies done during different months (January and late February-early March) of the northeast monsoon 2003 revealed a fivefold increase in the average euphotic zone integrated NO_3^- uptake from January (2.3 mmolN $m^{-2}d^{-1}$) to late February-early March (12.7 mmolN $m^{-2}d^{-1}$). The f-ratio during January appeared to be affected by the winter cooling effect and increased by more than 50% from the southernmost station to the northern open ocean stations, indicating hydrographic and meteorological control. Estimates of NO_3^- residence time suggested that NO_3^- entrained in the water column during January contributed to the development of blooms during late February-early March.

1. Introduction

The cycling of nitrogen (N) plays an important role in our environment and ecosystem. Primary production by photosynthesis is directly related to the N cycle and the productivity of many ecosystems is known to be controlled by N availability [1]. One of the important parameters in the N cycle of oceans is N uptake by phytoplankton, which depends on light and substrate availability [2] and acts as a regulator of primary and export production in the ocean.

The part of primary production that is supported by external nitrogenous inputs of upwelled, riverine or aeolian origin introduced in the euphotic zone is known as new production, whereas regenerated production is defined as that part of the primary production which sustains on recycled nutrients like NH_4^+ and urea, within the euphotic zone [3]. Classically, NO_3^- uptake is considered as new production and NH_4^+ (and urea) uptake as regenerated production. The fraction of the total N uptake that is new is called the f-ratio and represents the probability that a N atom is assimilated by phytoplankton due to new production; likewise (1-f) is the probability of assimilation by regenerated production [4]. Due to its inextricable link with the export production, the proper understanding of new production and nutrient regime of different oceanic regions is of utmost importance in the global carbon cycle [5, 6].

The Arabian Sea constitutes the northwestern (NW) part of the Indian Ocean and encompasses an area of around 6.2×10^6 km^2 [7]. Although the Arabian Sea is one of the smallest ocean basins, its unique geographical setting makes it an interesting site for biogeochemical studies. The uniqueness of the Arabian Sea lies in the influence of seasonally reversing monsoonal wind forcings on the biogeochemical cycling. The wind over the Arabian Sea blows from the northeast

(NE) during mid-November to February producing the NE monsoon (NEM) and reverses direction during June and starts blowing from the southwest (SW) giving rise to the SW monsoon (SWM), which persists until September. The transition periods such as October-November and March-May are known as Fall (FI) and Spring Intermonsoon (SI), respectively [8].

In general, the NEM is characterised by moderate strength, relatively cool, and dry winds [9]. The low relative humidity and lower air temperature compared to the sea surface temperature (SST) result into negative net heat flux, that is, net flux of heat from the ocean to the atmosphere leading to increased evaporation and surface salinity [10]. The dense saline surface water sinks causing convective mixing and consequently deepening of the mixed layer that erodes the nutricline. Dickey et al. [11] have observed seasonal mixed layer depth (MLD) as deep as 100–120 m during the NEM. Convective mixing has been observed in different parts of the Arabian Sea during the NEM [9, 12, 13] except regions adjacent to the coast of Oman [14].

The upwelling and convective mixing bring enormous amounts of nutrient rich deep water into the surface layer of the Arabian Sea, leading to increases in primary productivity. Primary productivity higher than 1.5 $gC\,m^{-2}\,d^{-1}$ during the NEM compared to 1.03 $gC\,m^{-2}\,d^{-1}$ during the SI has been measured in the western and the central Arabian Sea [15]. Madhupratap et al. [12] have reported a more than doubling in biological productivity from the SI (310 $mgC\,m^{-2}\,d^{-1}$) to the NEM (807 $mgC\,m^{-2}\,d^{-1}$) in the NE Arabian Sea.

The western and the NW parts of the Arabian Sea have been the focus of attention of scientists worldwide due to relatively high productivity and were studied thoroughly during JFOFS (Joint Global Ocean Flux Study, 1994–1996). The NE part, that is, off India, has also been studied for different physical, chemical, and biological parameters [12, 13, 16–18]. However, unlike the western and the NW Arabian Sea, which have been studied thoroughly for N-uptake dynamics, limited number of stations have been covered in the NE Arabian Sea in this regard [19–21].

During this study, we present NO_3^- and NH_4^+ uptake rates in the NE Arabian Sea during January 2003 and NO_3^- uptake rates during late February-early March 2003 (henceforth Feb-March). These two time periods (4–17th January and 28th February-5th March) are approximately the middle and waning phases of the NEM. We explore changes in N-uptake rates in short span of two months and compare the results with earlier studies from elsewhere in the Arabian Sea. We also deal with the effect of winter cooling on NO_3^- uptake and explore the modes of nutrient supply for the sustenance of phytoplankton blooms during Feb-March.

2. Material and Methods

Two cruises were undertaken to study N uptake rates in the NE Arabian Sea during the NEM, 2003. The first cruise was onboard ORV *Sagar Kanya* (SK-186) from 4–17th January and the second cruise was onboard FORV *Sagar Sampada* (SS-212) during Feb-March (28th February-5th March). The

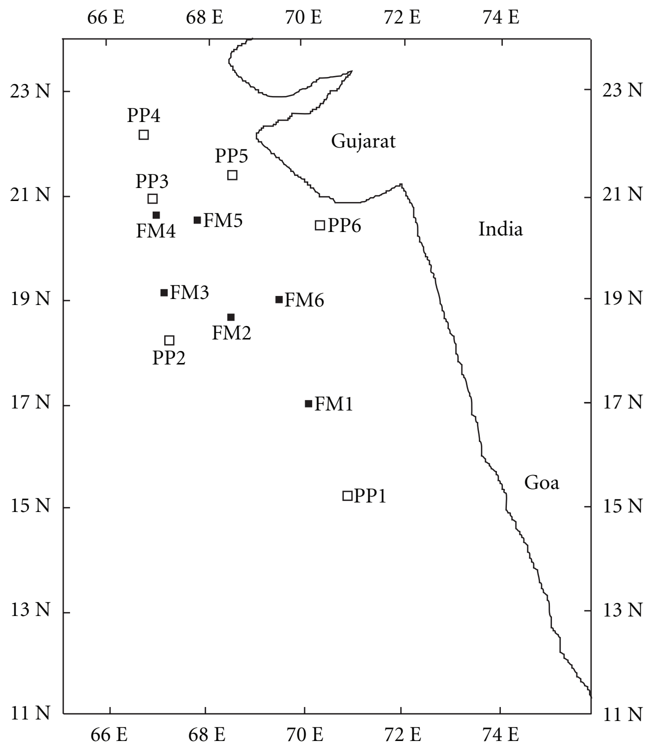

Figure 1: Location of stations during the present study. Open (PPs) and filled (FMs) squares are stations covered during January and late February-early March, respectively.

cruises did not follow the same tracks during both studies; however, they were mostly in the same region, that is, off Gujarat, India (Figure 1; Table 1). Six locations were covered during both cruises. Experiment at only one station was performed in a day. Four out of six stations during January were open ocean stations (PP1 to PP4) and two (PP5 and PP6) were coastal stations. During Feb-March all stations (FM1–FM6) were located in open ocean. Both NO_3^- and NH_4^+ uptake rates were measured during January, whereas only NO_3^- uptake rates could be measured during Feb-March as ambient NH_4^+ could not be measured during this period due to logistic reasons. Nutrients were measured using an autoanalyzer (SKALAR). The detection limits were 0.1 and 0.01 μM for NO_3^- and NH_4^+, respectively.

Water samples were collected from four to six depths at each station to cover the entire euphotic zone. To know the euphotic depth and the percentage of light at the depth of sampling (approximately 100, 80, 64, 20, 5, 1%), a Satlantic radiometer was operated at each station. Apart from the light regime, the radiometer set also provided information regarding water column temperatures. The attenuation of light in the water column was very fast with depth at stations FM3, FM4, and FM5 during Feb-March. These three stations will be considered as bloom stations as the analysis proceeds. It was difficult to differentiate between the corresponding depths for 100 and 80% light levels at these three stations given the length of Niskin bottles (~1 m). Because of this

Table 1: Euphotic zone integrated NO_3^- and NH_4^+ uptake rates, chl *a*, ambient NO_3^- and NH_4^+ concentrations along with mixed layer and euphotic depths at different stations during January and late February-early March.

	Stn.	Latitude (N)	Longitude (E)	NO_3^- Uptake (mmol N m^{-2} d^{-1})	NH_4^+ Uptake (mmol N m^{-2} d^{-1})	Chl (mg m^{-2})	NO_3^- (mmol m^{-2})	NH_4^+ (mmol m^{-2})	MLD (m)	Euphotic Depth (m)
January	PP1	15°14.05′	70°46.0′	1.77	10.00	26.39	150.52	4.24	48	70
	PP2	18°16.73′	67°12.63′	1.58	5.39	28.88	116.70	3.02	77	70
	PP3	20°57.66	66°54.41′	1.03	3.78	28.16	254.01	8.40	82	65
	PP4	22°12.16′	66°41.68′	2.51	7.72	31.84	212.86	4.90	111	65
	PP5	21°22.43′	68°11.85′	2.48	5.39	27.47	155.82	3.83	78	60
	PP6	20°26.25′	70°23.58′	4.25	6.14	ND	5.20	0.55	53	25
Late Feb-Early March	FM1	17°19.02′	70°11.82′	10.95	ND	36.60	174.04	ND	58	85
	FM2	18°48.33′	68°28.53′	10.14	ND	38.77	536.65	ND	64	85
	FM3	19°5.03′	66°51.82	18.31	ND	45.19	22.25	ND	53	42
	FM4	20°44.42′	66°58.82	23.22	ND	52.55	52.92	ND	46	44
	FM5	20°28.88′	67°30.24′	7.82	ND	45.37	132.23	ND	90	42
	FM6	18°57.71′	69°21.17′	5.71	ND	29.40	24.86	ND	71	58

limitation, the sampling at above mentioned three stations were performed only at four depths.

Water samples were collected in 2-L acid washed polycarbonate Nalgene bottles in duplicate for NH_4^+ and NO_3^- uptake rates measurements at each depth. To avoid contamination, samples were filled directly from the Niskin to the Nalgene bottles without using intermediate containers. Incubation bottles were covered immediately with dark cloth to avoid light shock to plankton. Samples were spiked with 99 atom% enriched $^{15}NH_4Cl$ and Na $^{15}NO_3$ to trace NH_4^+ and NO_3^- uptake rates, respectively. An attempt was made to add tracers around 10% of ambient concentrations. However, at a few depths additions were higher, particularly for NH_4^+ due to very low ambient concentrations. Following tracer addition, samples were incubated in an on-deck water bath after putting the appropriate neutral density filters to simulate the ambient light conditions inside the bottles. Temperature of the water bath was maintained by flowing surface seawater. Samples were filtered on precombusted (4 hours @ 400°C) 47 mm Whatman GF/F filters after four hours of incubation approximately symmetrical to local noon. Subsequently they were dried and stored for further mass spectrometric analysis. The analysis was performed using a CarloErba elemental analyser interfaced via Conflo III to a Finnigan Delta Plus mass spectrometer. The coefficient of variation observed for ^{15}N atom% in plankton samples incubated with the NO_3^- tracer was less than 1%, whereas it was less than 4% for samples incubated with NH_4^+ tracer. The variability in particulate organic N (PON) for duplicate samples was less than 10%. The equation of Dugdale and Wilkerson [22] was used for uptake rates calculation. Daily uptake rates were calculated by multiplying hourly values by 12 for NO_3^- and by 18 for NH_4^+ [22, 23]. Column-integrated uptake rates were calculated using the trapezoidal integration method from the surface to the euphotic depth. We considered the sum of NO_3^- and NH_4^+ uptake rates as the total N uptake and the ratio of the column-integrated NO_3^- uptake to the column-integrated total N uptake as the *f*-ratio. No time-course experiments were performed to correct NH_4^+ uptake rates for isotope dilution [24], which could have led to underestimation of the NH_4^+ uptake rates during the present study [19]. Also, precise nanomolar level measurement of ambient NH_4^+ concentration could further improve the accuracy of NH_4^+ uptake. Therefore, given these methodological considerations, NH_4^+ uptake, and consequently the *f*-ratio, presented here may be considered as “approximate” rather than “actual”.

Chlorophyll *a* was estimated immediately using standard fluorometric method involving 90% acetone extraction [25].

3. Results

3.1. Meteorological and Hydrographic Conditions. In general, the Arabian Sea witnesses a SST difference from the south to the north (north being cooler) during the NEM. During January 2003, the maximum SST of 28.6°C was observed at the southernmost station (PP1) and the minimum of 24.9°C at the northernmost station (PP4; Figure 2(a)). In this region, the SST has been found to decrease at a rate of 0.5°C per degree latitude during winter [12]. The SST pattern during Feb-March was almost similar to January, that is, decreasing SST from the south to the north (Figure 2(a)). Zonal variability in SST (FM3 and FM6, FM4 and FM5) was also seen during this period. Air temperature at all the stations during the study period was less than the local SSTs by at least 0.5°C (figure not shown).

The depth profiles of temperature during January suggested a general increase in the MLD from the south to the north (Figure 2(b); Table 1). During the present study, the MLD is defined as the depth where the water temperature is 1°C less than the SST [13]. These MLD estimates are based on temperature profiles taken during noon and are not the daily average. During January, the MLD increased from 48 m at the southernmost station PP1 to 111 m at the northernmost PP4 (Figure 2(b); Table 1). At a few stations

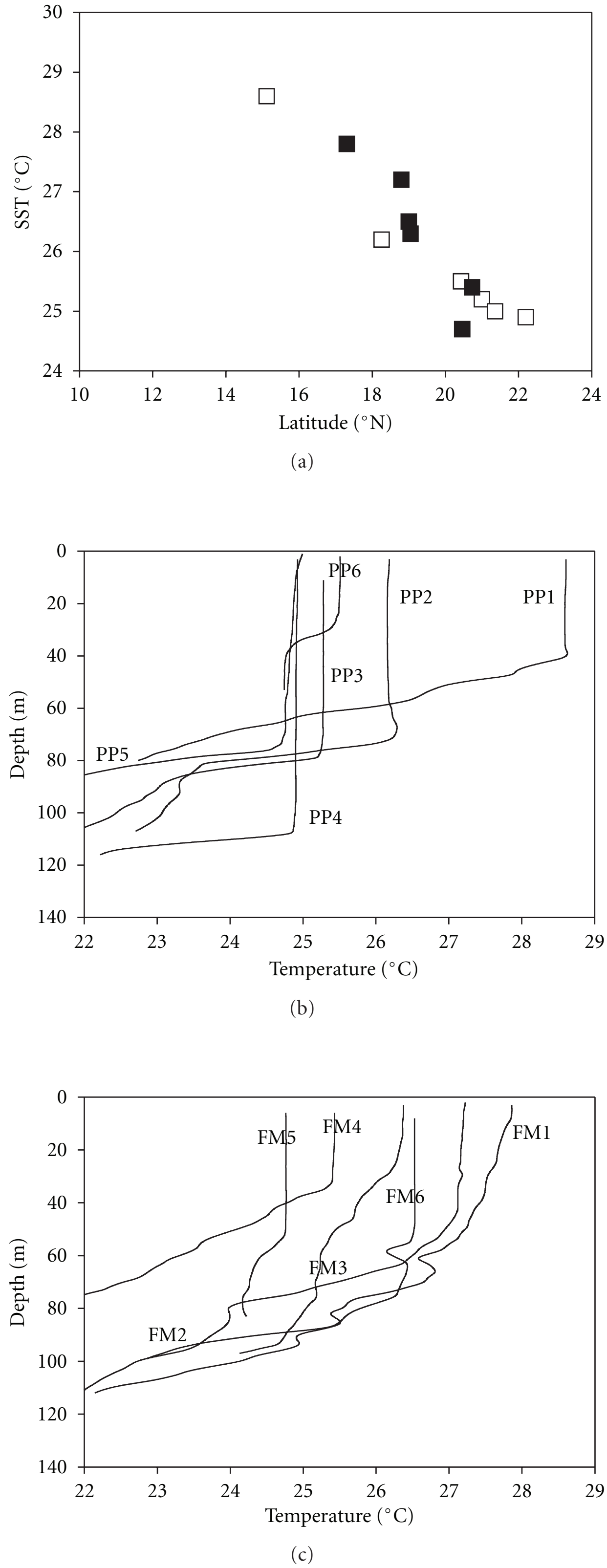

Figure 2: Thermal condition during sampling: (a) Sea surface temperature during January (open) and late February-early March (filled), (b) temperature profiles at different stations during January, and (c) temperature profiles at different stations during late February-early March.

in the same region (18–22 °N), the MLDs during Feb-March were relatively shallower compared to January (Figure 2(c); Table 1). This relative shoaling of the MLD from January to Feb-March may indicate a decrease in the effectiveness of winter cooling. However, marked diurnal variability in the MLD has also been noted towards the end of the winter monsoon due to large diurnal oscillation of net air-sea heat flux [9, 26].

Average wind speed with dominant direction was obtained from the shipboard instrument during the study period. The dominant wind direction during the entire study period was north/northeasterly with an average speed of around $4\,\mathrm{m\,s^{-1}}$ during January. During Feb-March, wind speeds at the first two stations were around 4.01 and $2.74\,\mathrm{m\,s^{-1}}$, respectively, typically in the range observed during January. However, it was more than $8\,\mathrm{m\,s^{-1}}$ at other stations. The observations and estimates based on QuikSCAT wind data reported in a concurrent satellite-based study [27] have been used for analysing the wind-driven processes during the study period. The average euphotic depth observed at each station during the study period is shown in Table 1.

3.2. Nutrients and Chlorophyll. The vertical profiles of NO_3^- at different stations during January suggested relatively low NO_3^- in the upper 40 m of the water column (<0.5 μM) at the southernmost station (PP1), which increased to >1.2 μM at majority of the northern stations (Figure 3(a)). At the coastal station PP6, it decreased significantly (<0.3 μM). The NO_3^- profiles during Feb-March (Figure 3(b)) also indicated relatively low NO_3^- in the top 60 m at the southern station FM1. It was low in the top 25 m at FM2 but increased significantly at the base of euphotic zone. The NO_3^- concentration was considerably higher throughout the water column at the northern stations FM4 (>1 μM) and FM5 (>2.5 μM). One important difference between the bloom and the nonbloom stations during Feb-March was relatively higher NO_3^- in the surface layer at the bloom stations. The NH_4^+ concentrations during January were never more than 0.2 μM within the euphotic zone and they were below detection limit at some depths (Figure 3(c)).

Chlorophyll *a* during January varied from $0.24\,\mathrm{mg\,m^{-3}}$ (45 m at PP5) to $0.76\,\mathrm{mg\,m^{-3}}$ (surface at PP5). No distinctive subsurface maxima, except at PP5 (30 m), were observed (Figure 4(a)). We do not have chlorophyll *a* data for PP6. During Feb-March, wide variation in chlorophyll *a* (0.08 to $1.6\,\mathrm{mg\,m^{-3}}$) with significantly higher values at the bloom stations compared to the nonbloom stations were observed (Figure 4(b)). Chlorophyll *a* at the bloom stations were around or more than $1\,\mathrm{mg\,m^{-3}}$ (except FM5 at surface ~ $0.6\,\mathrm{mg\,m^{-3}}$) in the top 42 m and decreased considerably below that. Subsurface maxima at the base of euphotic zone (~42 m) at FM3 and FM4 and at 20 m at FM5 were seen. The reason for higher chlorophyll *a* near the euphotic depth is not clear to us. At nonbloom stations chlorophyll *a* was mostly less than $0.7\,\mathrm{mg\,m^{-3}}$, in the similar range as observed during January.

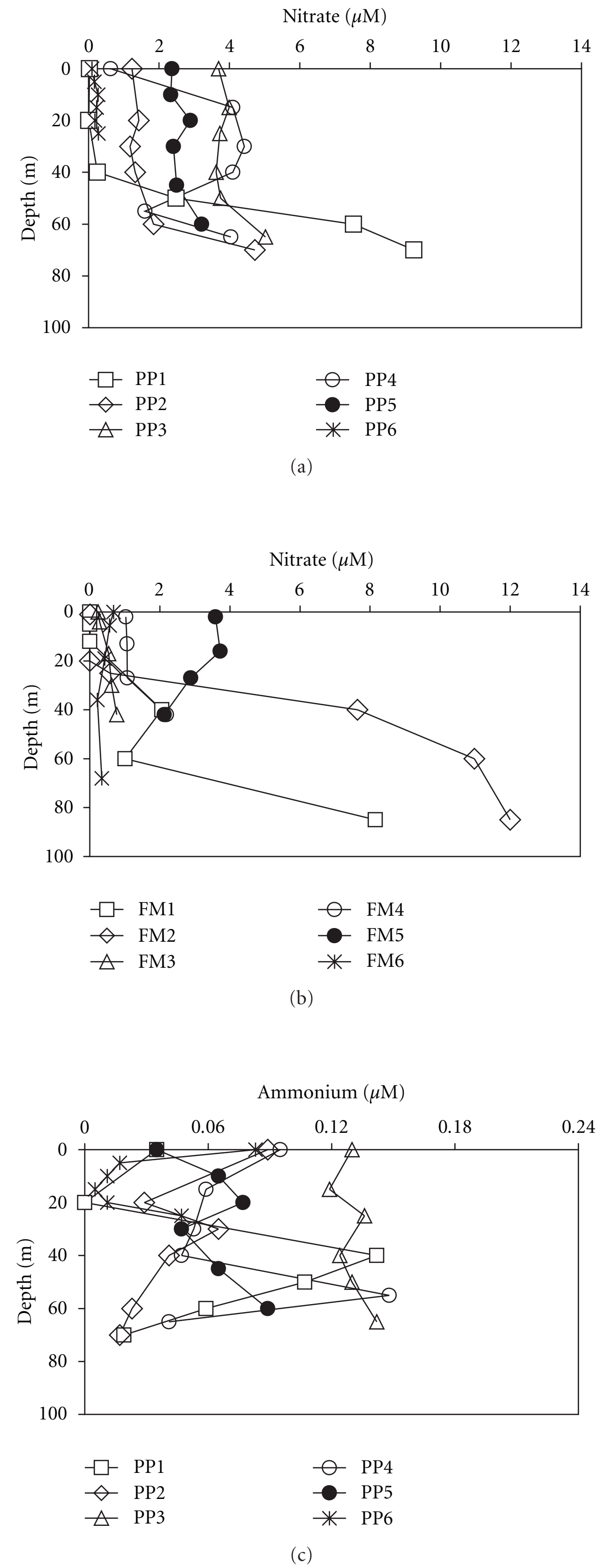

Figure 3: Nutrient availability during sampling. Depth profiles of (a) NO_3^-—January, (b) NO_3^-—late February-early March, and (c) NH_4^+—January.

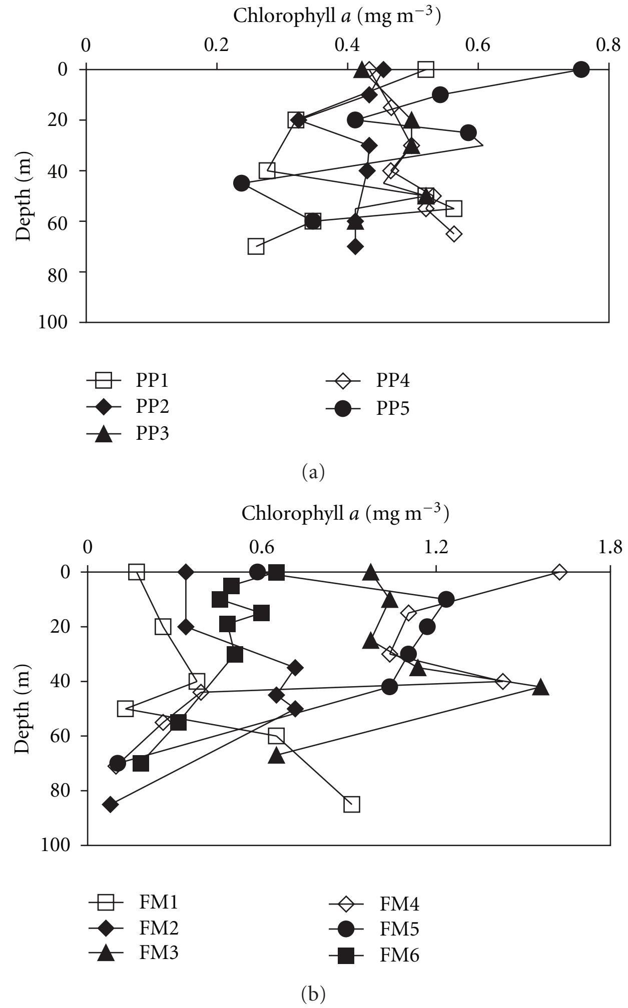

Figure 4: Depth profiles of chlorophyll *a* during (a) January, and (b) late February-early March.

3.3. N Uptake Rates. The total ($NO_3^- + NH_4^+$), NO_3^-, and NH_4^+ uptake rates along with the *f*-ratio are discussed for January, whereas only NO_3^- uptake is discussed for Feb-March.

3.3.1. Total Uptake. Euphotic zone integrated total N uptake rates ranged from 4.8 to 11.8 mmol N m^{-2} d^{-1} and averaged around 8.7 ($\pm$2.6) mmol N m^{-2} d^{-1} ($n = 6$) during January. Station-wise NO_3^- and NH_4^+ uptake rates are shown in Table 1. The highest rate was observed at the southernmost station PP1 and the lowest was at PP3, both open ocean stations. No systematic spatial variation from the south to the north was observed. The average rate for open ocean stations was around 8.4 ($\pm$3.1) mmol N m^{-2} d^{-1} and two coastal stations averaged around 9.1 ($\pm$1.8) mmol N m^{-2} d^{-1}. The numbers in parentheses represent spatial variability. The uncertainties arising from the methodological considerations mentioned earlier may also introduce uncertainties in spatial variability.

3.3.2. NO_3^- Uptake

January. Euphotic zone integrated NO_3^- uptake rates during January ranged from 1.0 to 4.2 mmol N m^{-2} d^{-1} with an average of 2.3 mmol N m^{-2} d^{-1} (station-wise data shown in Table 1 with latitude-wise presentation in Figure 5(a)). Values at open ocean locations averaged around 1.7 mmol N m^{-2} d^{-1} and average of two coastal stations (3.4 mmol N m^{-2} d^{-1}) was twice that of the former (Figure 5(a)). This higher average value at the coastal locations was mainly due to the NO_3^- uptake observed at PP6 (4.2 mmol N m^{-2} d^{-1}), the highest during January. PP6 was closest to the coast and had shallowest euphotic depth (~25 m) with virtually no NO_3^- in the euphotic zone (~5.2 mmol m^{-2}) compared to other locations (>115 mmol m^{-2}; Table 1), probably indicating the utilization of available NO_3^- by phytoplankton at this location.

Late February-Early March. Euphotic zone integrated NO_3^- uptake rates during Feb-March ranged from 5.7 mmol N m^{-2} d^{-1} at a nonbloom station (FM6) to 23.2 mmol N m^{-2} d^{-1} at a bloom station (FM4; Table 1 and Figure 5(b)). The average column NO_3^- uptake was 12.7 mmol N m^{-2} d^{-1}, more than five times that of observed during January (2.3 mmol N m^{-2} d^{-1}). The average NO_3^- uptake at the bloom stations was 16.4 mmol N m^{-2} d^{-1}, almost twice that of the nonbloom stations average (8.9 mmol N m^{-2} d^{-1}).

The increase in average NO_3^- uptake from January to Feb-March for the same region (18–22 °N) remains five-fold (2.3 to 13.0 mmol N m^{-2} d^{-1}). This temporal increase in NO_3^- uptake rate coincided with the significant decrease in euphotic zone integrated NO_3^- concentration at some stations during Feb-March. This was also reflected in increased biomass concentrations. Euphotic zone integrated chlorophyll *a* was considerably higher during Feb-March, particularly at three bloom stations (>45 mg m^{-2}; Table 1). At FM5, the euphotic zone integrated chlorophyll *a* was one of the highest with a typical bloom station euphotic depth of 42 m, but NO_3^- uptake (7.8 mmol N m^{-2} d^{-1}) was significantly lower compared to other two bloom stations (Table 1; Figure 5(b)). The reason for this is unknown to us. The NO_3^- uptake rate at bloom station FM4 (23.2 mmol N m^{-2} d^{-1}) is the highest estimate of NO_3^- uptake reported for the Arabian Sea so far.

3.3.3. NH_4^+ Uptake. Euphotic zone integrated NH_4^+ uptake rates during January varied from 3.8 to 10 mmol N m^{-2} d^{-1} with an overall average of 6.4 mmol N m^{-2} d^{-1}. There was no considerable difference between the average uptake rates at open (6.7 mmol N m^{-2} d^{-1}) and coastal (5.8 mmol N m^{-2} d^{-1}) locations. The lowest NH_4^+ uptake was observed at PP3 where NO_3^- uptake was also the lowest (Figure 5(a)), but euphotic zone integrated chlorophyll *a* was in the same range as other stations (Table 1).

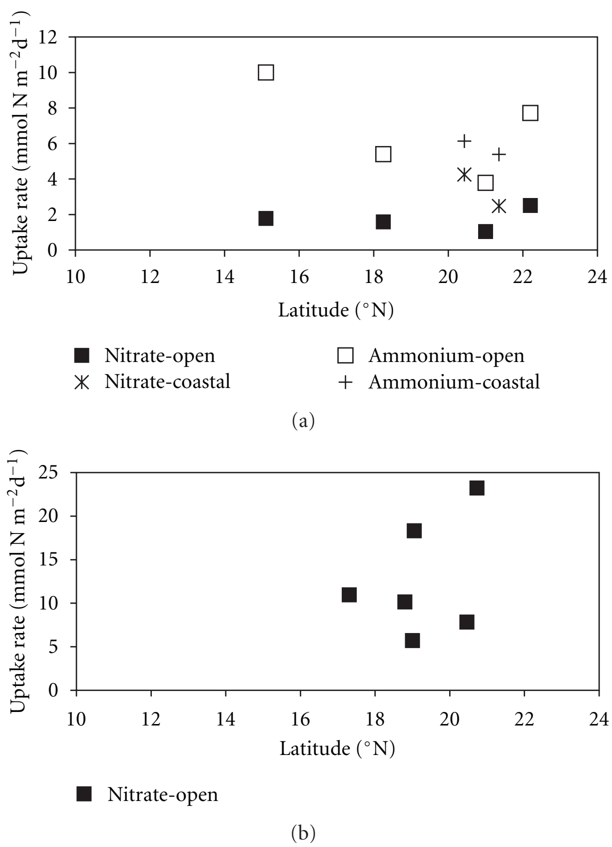

Figure 5: Euphotic zone integrated (a) NO_3^- and NH_4^+ uptake rates during January, and (b) NO_3^- uptake rates during late February-early March.

3.3.4. Vertical Profiles. The vertical profiles of uptake rates at different stations suggested subsurface NO_3^- uptake maxima in the top 20 m for two coastal locations (PP5 and PP6) and an open ocean location (PP4) during January (Figure 6(a)). The southernmost station PP1 showed NO_3^- uptake maxima at 40 m. No such distinct maxima were observed in biomass concentrations at these depths on these locations. The NO_3^- uptake in the top 15 m was quite high at PP6 compared to other locations during January. Subsurface maxima for NH_4^+ uptake were observed around 10 m at PP5 and around 42 m at PP1 (Figure 6(b)). Similar to NO_3^- uptake, NH_4^+ uptake was also quite high in the top 15 m at PP6. Two bloom stations (FM 3 and FM 5) during Feb-March showed NO_3^- uptake maxima in the top 20 m. FM4 showed highest uptake on the surface and nonbloom station FM1 at around 40 m (Figure 6(c)). Both NO_3^- and NH_4^+ uptake rates decreased with depth but did not appear to cease completely at the bottom of the euphotic zone.

3.3.5. f-Ratio. The overall variation in *f*-ratio (NO_3^- uptake: total N uptake) was from 0.15 at PP1 to 0.40 at PP6 with an average of 0.26 (latitude-wise data shown in Figure 7). The open ocean stations averaged around 0.21, whereas two coastal stations averaged around 0.36.

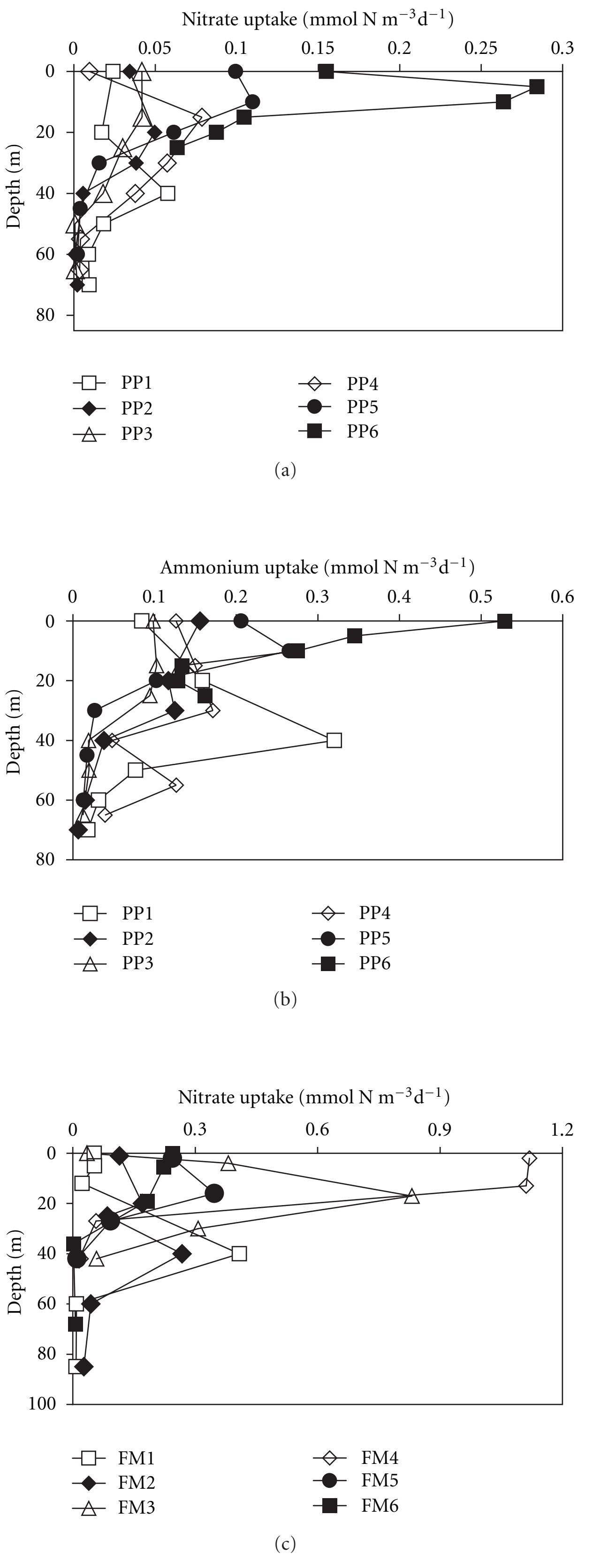

FIGURE 6: Vertical profiles of (a) NO_3^- uptake rates during January, (b) NH_4^+ uptake rates during January, and (c) NO_3^- uptake rates during late February-early March.

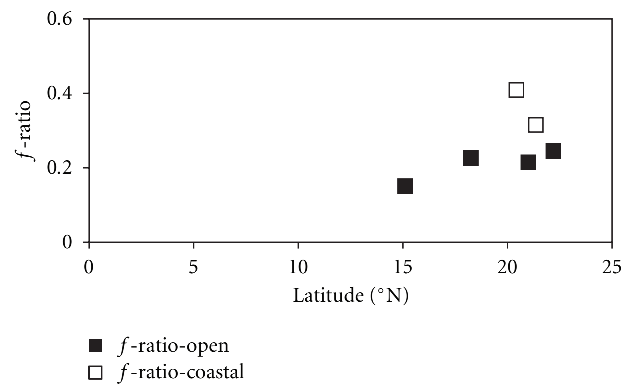

FIGURE 7: f-ratios during January.

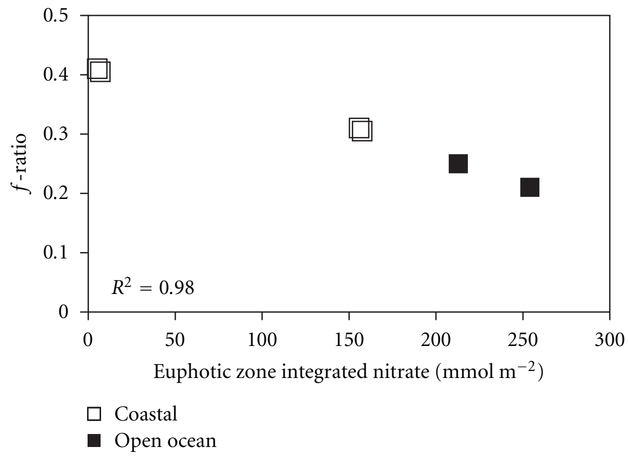

FIGURE 8: Relationship between f-ratio and euphotic zone integrated NO_3^- within ~ 20–22 °N during January.

To minimize the effect of north-south variability in meteorological conditions, analysis of f-ratios within a relatively narrow spatial region (~20–~22 °N; PP3–PP6) was performed. This analysis revealed a significant negative correlation ($R^2 = 0.98$) between euphotic zone integrated NO_3^- and f-ratio, that is, lower f-ratio in open ocean compared to coastal locations despite higher euphotic zone integrated NO_3^- (Figure 8), possibly indicating the underutilization of NO_3^- in the open ocean. The relationship remained significant even after inclusion of PP2 ($R^2 = 0.71$).

Although there are limited numbers of stations, a noticeable increase in f-ratio from the southernmost station (PP1: 0.15) to the northern stations (PP2–PP4: 0.21–0.24) was observed in the open ocean (Figure 7). This is consistent with the decreasing SST and increasing MLD from the south to the north.

4. Discussion

The proper understanding of the N uptake dynamics of an oceanic region is important to decipher its N cycle.

The present study, with its focus on the NE Arabian Sea during the middle and the waning phases of the NEM, intended to explore the changes in N uptake potential within this relatively unexplored region. There were limited numbers of stations in this region during JGOFS [N7–N11, 19; N7-N8, 21] and ARABESQUE [A9/2, 20]. Although not directly comparable due to interannual variability and differences in methodological and measurement techniques, we have confined only to the above-mentioned stations of the previous studies for comparison with our stations in the same region (PP2–PP4 during January and FM2-FM5 during Feb-March).

The average NO_3^- uptake rate for January (PP2–PP4 ∼ 1.7 mmol N m^{-2} d^{-1}) during the present study is close to the average NO_3^- uptake rate reported by McCarthy et al. [19] for the same month (N7–N11 ∼ 1.5 mmol N m^{-2} d^{-1}). However, the average NO_3^- uptake rate for Feb-March (FM2–FM5 ∼ 14.9 mmol N m^{-2} d^{-1}) during the present study is significantly higher than previously reported values in the region. Prior to the present study, the highest NO_3^- uptake rate in the Arabian Sea was reported by Watts and Owens [20] at their station A9/2 (9.8 mmol N m^{-2} d^{-1}) during November-December. This station is close to PP1 of the present study but has significantly higher NO_3^- uptake rate, which may be due to temporal or methodological differences.

The average NH_4^+ uptake rate during the present study (PP2–PP4 ∼5.6 mmol N m^{-2} d^{-1}) is considerably lower than the average value reported by McCarthy et al. [19] for January (N7–N11 ∼ 25 mmol N m^{-2} d^{-1}). This could be due to potential underestimation of NH_4^+ uptake rates during the present study due to the lack of isotope dilution correction. However, A9/2 (8.3 mmol N m^{-2} d^{-1}) had similar NH_4^+ uptake as PP1 (9.9 mmol N m^{-2} d^{-1}). Due to lower NH_4^+ uptake rates, the average *f*-ratio during the present study (PP2–PP4 ∼ 0.23) is higher compared to McCarthy et al. [19] (N7–N11 ∼ 0.06).

At all stations during January, NH_4^+ uptake was higher compared to NO_3^- uptake and primary production was dominantly supported by NH_4^+ based regenerated N (*f*-ratio ∼0.26), similar to the observations from other studies [19–21]. Due to limited data and different aim of the present study, it is not possible to clearly decipher whether this higher NH_4^+ uptake was due to relative preference of NH_4^+ by phytoplankton or due to inhibition of NO_3^- uptake by the presence of NH_4^+. The preference for reduced (recycled) forms of N such as NH_4^+ is well known in aquatic environments [3, 28–30] due to higher energy requirement for the assimilation of NO_3^- [31]. Inhibition of NO_3^- uptake due to NH_4^+ has also been reported [32].

The lower *f*-ratios at open ocean locations compared to coastal locations and observed negative relationship between euphotic zone integrated NO_3^- and *f*-ratio (Figure 8) suggest limited NO_3^- utilization in open ocean despite higher NO_3^- availability, possibly due to some physical or biological controls. Suppression of NO_3^- uptake in the presence of NH_4^+ [19, 29, 30, 33] or higher than required addition of $^{15}NH_4^+$ tracer during the experiments, which can trigger artificial stimulation of NH_4^+ uptake [20], could be possible reasons for lower *f*-ratio. However, during the present study, the addition of $^{15}NH_4^+$ was not large enough to stimulate the artificial uptake as evidenced by absence of correlation (R^2 ∼ 0.006; figure not shown) between the percentages of NH_4^+ addition relative to ambient and NH_4^+ uptake rates.

Another possible reason for limited NO_3^- utilization could be iron and silicon limitation [34]. However, the ranges of iron [35] and silica [14] concentrations are greater than known limiting values in the Arabian Sea during the NEM. Some recent studies suggested combined effect of microzooplankton grazing and diurnal cycling of mixed layer to be another important factor in limited nutrient utilization [36–38]. However, we do not have data to independently verify this during the present study.

The increase in *f*-ratio from the southernmost station (PP1) to the northern stations shows the hydrographic and meteorological control on *f*-ratio (Figure 7). Platt et al. [39] have observed that in areas where surface layers are strongly coupled with subsurface layers, new production is a significant fraction of the total production. Deeper mixed layers and high NO_3^- concentrations in the water column at most of the northern stations during January indicate surface-subsurface coupling during the present study (Figures 2 and 3). Similar observations have been made elsewhere in the NE Arabian Sea during winter [12, 13].

The possible reasons for high NO_3^- concentration in the water column at most of the stations during January could be convective mixing due to winter cooling and/or upwelling under the influence of wind. Based on wind speed, specific humidity [40], and computation of heat and freshwater (Evaporation-Precipitation) fluxes, Madhupratap et al. [12] found convective mixing due to winter cooling to be the most likely reason for the deepening of mixed layers and high nutrient concentrations in the water column of the NE Arabian Sea during winter. Similarities in physical conditions and nitrate concentrations between previous [12, 13] and the present study suggest that winter convection was most likely active during the present study as well. However, calculations performed by a satellite-based study conducted concurrently to the present study also found an evidence of upward Ekman pumping during the study period (PP3; < 0.5 m d^{-1}) [27]. It appears that Ekman pumping could be a supplementary factor causing the upward transport of nutrients besides the winter convection-based entrainment [27]. Overall, the trend in SSTs, midday MLDs, and NO_3^- concentrations during January suggest that the winter cooling/upwelling effect was relatively prevalent in the northern part of the study region than the southern, which probably led to relative increase in the *f*-ratio in the northern region.

Within the same geographical area (18–22 °N), the average NO_3^- uptake during Feb-March was more than five-fold higher than January. The analysis of sources of NO_3^- available for this high uptake during Feb-March is important. Although the midday temperature profiles during Feb-March indicate relatively shorter MLDs, large diurnal variation in MLDs during this period is known in the Arabian Sea [11, 26]. The lack of diurnal MLDs data during the present study restricts us from predicting the dynamics of nutrient replenishment in the water column by this process, but it may be a possible nutrient source. The calculations based on QuikSCAT wind data (at FM4) suggest a strong upwelling event during the first week of March 2003 (i.e., study period) with the highest upward vertical velocity of water mass (~1 m d^{-1}) on 3rd March [27], indicating a different way of nutrient entrainment in the water column. Another important source of NO_3^- during Feb-March could be the NO_3^- entrained in the water column during January.

Despite higher NO_3^- concentration in the water column, the relatively lower NO_3^- uptake during January compared to Feb-March indicates incomplete utilization of entrained NO_3^- during January. Residence time of NO_3^- in the water column was estimated by dividing the midday euphotic zone integrated NO_3^- concentrations with the daily NO_3^- uptake rates. Residence time of NO_3^- was more than 60 days during January, whereas it was shorter (<20 d) at most of the stations during Feb-March (Figure 9). This is the minimum estimate of NO_3^- residence time as any additional NO_3^- supplied during the period under consideration was ignored. Also, any possible replenishment of NO_3^- due to deepening of the MLD during night might lead to higher daily integrated NO_3^- compared to the midday values used during the present calculation. The NO_3^- residence times seemed to be independent of MLDs and assuming the same rate of continued removal due to uptake by phytoplankton, NO_3^- entrained during January would remain in the water column for at least 60 days indicating its possible availability during Feb-March.

In general, NO_3^- entrained in the water column through different processes like, winter convection and wind driven Ekman pumping, appears to be source for high NO_3^- uptake during Feb-March. Similar to observations made by Banse and English [41], there appears to be a time lag between the nutrient entrainment and peak biomass development during the present study as well. The temporal trend of satellite chlorophyll data from OCM (Ocean Colour Monitor; at PP3) shows decline in chlorophyll concentration after first week of January to peak again during Feb-March [27]. The availability of NO_3^- along with increased light conditions due to relatively shallower MLDs possibly triggered the development of a bloom or high NO_3^- uptake [42]. The NO_3^- uptake rates during two different periods, residence time of NO_3^- entrained during January, and temporal trend of satellite-based chlorophyll data suggest that there was a time lag between NO_3^- entrainment and peak uptake of NO_3^- during the present study. McCarthy et al. [19] have also observed disparity between entrainment and uptake rates of NO_3^-, which lead to turnover times of 1 to 3 months over the NEM.

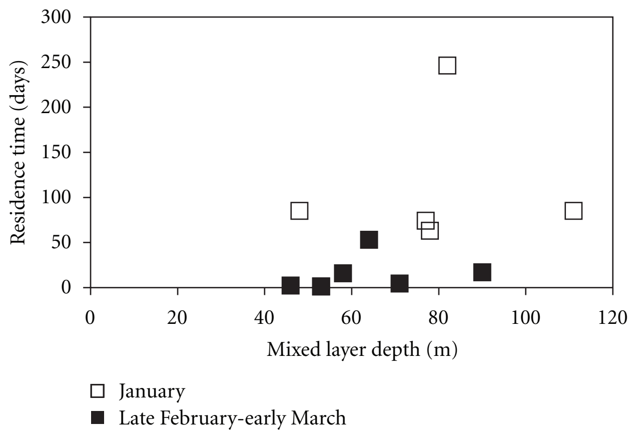

Figure 9: Residence time of NO_3^- in the water column and its relation with the MLD.

5. Conclusions

The present study was an attempt to quantify NO_3^- and NH_4^+ uptake rates in the NE Arabian Sea during the middle and the waning phases of the NEM. The effect of winter cooling on the f-ratio and increase in NO_3^- uptake during waning phase of the NEM were the major focus of the study. A preliminary evidence of hydrographic and meteorological control on the f-ratio as observed by the increase in f-ratio from the south to the north was found. However, we recommend additional experiments with extensive physical data to ascertain this evidence. NO_3^- uptake during the bloom in late February-early March was five-fold higher than the NO_3^- uptake in January. Nutrients entrained in the water column during the middle phase of the NEM (January) along with upwelled nutrients due to Ekman pumping appear to be possible source for the development of blooms during the waning phase (late February-early March).

Acknowledgments

The authors thank Dr. M. Sudhakar and Department of Ocean Development for ship time for this work, funded by ISRO-GBP Department of Space, Government of India. They thank participants and crews of the cruises *ORV Sagar Kanya*-186 and *FORV Sagar Sampada*-212 for their help, S.W. A. Naqvi for arranging nutrient analysis.

References

[1] P. M. Vitousek, S. Hattenschwiler, L. Olander, and S. Allison, "Nitrogen and nature," *Ambio*, vol. 31, no. 2, pp. 97–101, 2002.

[2] J. J. MacIsaac and R. C. Dugdale, "Interactions of light and inorganic nitrogen in controlling nitrogen uptake in the sea," *Deep-Sea Research and Oceanographic Abstracts*, vol. 19, no. 3, pp. 209–232, 1972.

[3] R. C. Dugdale and J. J. Goering, "Uptake of new and regenerated forms of nitrogen in primary productivity," *Limnology & Oceanography*, vol. 12, pp. 196–206, 1967.

[4] R. W. Eppley and B. J. Peterson, "Particulate organic matter flux and planktonic new production in the deep ocean," *Nature*, vol. 282, no. 5740, pp. 677–680, 1979.

[5] P. G. Falkowski, E. A. Laws, R. T. Barber, and J. W. Murray, "Phytoplankton and their role in primary, new, and export production," in *Ocean Biogeochemistry*, M. J. Fasham, Ed., pp. 99–121, Springer, Berlin, Germany, 2003.

[6] J. L. Sarmiento, J. Dunne, and R. A. Armstrong, "Do we understand the ocean's biological pump," *USJGOFS News*, vol. 12, no. 4, pp. 1–5, 2005.

[7] P. H. Burkill, R. F. C. Mantoura, and N. J. P. Owens, "Biogeochemical cycling in the northwestern Indian Ocean: a brief overview," *Deep-Sea Research Part II*, vol. 40, no. 3, pp. 643–649, 1993.

[8] S. L. Smith, L. A. Codispoti, J. M. Morrison, and R. T. Barber, "The 1994–1996 Arabian Sea Expedition: an integrated, interdisciplinary investigation of the response of the northwestern Indian Ocean to monsoonal forcing," *Deep-Sea Research Part II*, vol. 45, no. 10-11, pp. 1905–1915, 1998.

[9] R. A. Weller, M. F. Baumgartner, S. A. Josey, A. S. Fischer, and J. C. Kindle, "Atmospheric forcing in the Arabian Sea during 1994-1995: observations and comparisons with climatology and models," *Deep-Sea Research Part II*, vol. 45, no. 10-11, pp. 1961–1999, 1998.

[10] R. A. Weller, A. S. Fischer, D. L. Rudnick, et al., "Moored observations of upper-ocean response to the monsoons in the Arabian Sea during 1994-1995," *Deep-Sea Research Part II*, vol. 49, no. 12, pp. 2195–2230, 2002.

[11] T. Dickey, J. Marra, D. E. Sigurdson, et al., "Seasonal variability of bio-optical and physical properties in the Arabian Sea: October 1994-October 1995," *Deep-Sea Research Part II*, vol. 45, no. 10-11, pp. 2001–2025, 1998.

[12] M. Madhupratap, S. Prasanna Kumar, P. M. A. Bhattathiri, et al., "Mechanism of the biological response to winter cooling in the northeastern Arabian Sea," *Nature*, vol. 384, no. 6609, pp. 549–552, 1996.

[13] S. Prasanna Kumar, N. Ramaiah, M. Gauns, et al., "Physical forcing of biological productivity in the Northern Arabian Sea during the Northeast Monsoon," *Deep-Sea Research Part II*, vol. 48, no. 6-7, pp. 1115–1126, 2001.

[14] J. M. Morrison, L. A. Codispoti, S. Gaurin, B. Jones, V. Manghnani, and Z. Zheng, "Seasonal variation of hydrographic and nutrient fields during the US JGOFS Arabian Sea Process Study," *Deep-Sea Research Part II*, vol. 45, no. 10-11, pp. 2053–2101, 1998.

[15] R. T. Barber, J. Marra, R. C. Bidigare, et al., "Primary productivity and its regulation in the Arabian Sea during 1995," *Deep-Sea Research Part II*, vol. 48, no. 6-7, pp. 1127–1172, 2001.

[16] S. R. Shetye, A. D. Gouveia, and S. S. C. Shenoi, "Hydrography and circulation off the west coast of India during Southwest Monsoon 1987," *Journal of Marine Research*, vol. 48, pp. 359–378, 1990.

[17] P. M. A. Bhattathiri, A. Pant, S. Sawant, M. Gauns, S. G. P. Matondkar, and R. Mohanraju, "Phytoplankton production and chlorophyll distribution in the eastern and central Arabian Sea in 1994-1995," *Current Science*, vol. 71, no. 11, pp. 857–862, 1996.

[18] N. Ramaiah, S. Raghukumar, and M. Gauns, "Bacterial abundance and production in the central and eastern Arabian Sea," *Current Science*, vol. 71, no. 11, pp. 878–882, 1996.

[19] J. J. McCarthy, C. Garside, and J. L. Nevins, "Nitrogen dynamics during the Arabian Sea Northeast Monsoon," *Deep-Sea Research Part II*, vol. 46, no. 8-9, pp. 1623–1664, 1999.

[20] L. J. Watts and N. J. P. Owens, "Nitrogen assimilation and the f-ratio in the northwestern Indian Ocean during an intermonsoon period," *Deep-Sea Research Part II*, vol. 46, no. 3-4, pp. 725–743, 1999.

[21] R. N. Sambrotto, "Nitrogen production in the northern Arabian Sea during the Spring Intermonsoon and Southwest Monsoon seasons," *Deep-Sea Research Part II*, vol. 48, no. 6-7, pp. 1173–1198, 2001.

[22] R. C. Dugdale and F. P. Wilkerson, "The use of ^{15}N to measure nitrogen uptake in eutrophic oceans; experimental considerations," *Limnology & Oceanography*, vol. 31, no. 4, pp. 673–689, 1986.

[23] R. C. Dugdale, F. P. Wilkerson, R. T. Barber, and F. P. Chavez, "Estimating new production in the equatorial Pacific Ocean at 150°W," *Journal Geophysical Research*, vol. 97, pp. 681–686, 1992.

[24] E. Laws, "Isotope dilution modeled and the mystery of the vanishing ^{15}N," *Limnology & Oceanography*, vol. 29, pp. 379–386, 1984.

[25] N. A. Welschmeyer, "Fluorometric analysis of chlorophyll a in the presence of chlorophyll b and pheopigments," *Limnology & Oceanography*, vol. 39, no. 8, pp. 1985–1992, 1994.

[26] C. de Boyer Montégut, G. Madec, A. S. Fischer, A. Lazar, and D. Iudicone, "Mixed layer depth over the global ocean: an examination of profile data and a profile-based climatology," *Journal of Geophysical Research C*, vol. 109, no. 12, pp. 1–20, 2004.

[27] R. M. Dwivedi, M. Raman, K. N. Babu, S. K. Singh, N. K. Vyas, and S. G. P. Matondkar, "Formation of algal bloom in the northern Arabian Sea deep waters during January–March: a study using pooled in situ and satellite data," *International Journal of Remote Sensing*, vol. 29, no. 15, pp. 4537–4551, 2008.

[28] J. J. McCarthy and R. W. Eppley, "A comparison of chemical isotopic and enzymatic methods for measuring nitrogen assimilation of marine phytoplankton," *Limnology & Oceanography*, vol. 17, pp. 371–382, 1972.

[29] P. M. Glibert, D. C. Biggs, and J. J. McCarthy, "Utilization of ammonium and nitrate during austral summer in the Scotia Sea," *Deep Sea Research Part A*, vol. 29, no. 7, pp. 837–850, 1982.

[30] A. P. Rees, N. J. P. Owens, M. R. Heath, D. H. Plummer, and R. S. Bellerby, "Seasonal nitrogen assimilation and carbon fixation in a fjordic sea loch," *Journal of Plankton Research*, vol. 17, no. 6, pp. 1307–1324, 1995.

[31] J. J. McCarthy and E. J. Carpenter, "Nitrogen cycling in near surface waters of the open ocean," in *Nitrogen in the Marine Environment*, E. J. Carpenter and D. G. Capone, Eds., pp. 487–512, Academic Press, New York, NY, USA, 1983.

[32] Q. Dortch, "The interaction between ammonium and nitrate uptake in phytoplankton," *Marine Ecology Progress Series*, vol. 61, pp. 183–201, 1990.

[33] W. G. Harrison, T. Platt, and M. R. Lewis, "f-ratio and its relationship to ambient nitrate concentration in coastal waters," *Journal of Plankton Research*, vol. 9, pp. 235–248, 1987.

[34] M. R. Landry, R. T. Barber, R. R. Bidigare, et al., "Iron and grazing constraints on primary production in the central equatorial Pacific: an EqPac synthesis," *Limnology & Oceanography*, vol. 42, no. 3, pp. 405–418, 1997.

[35] C. I. Measures and S. Vink, "Seasonal variations in the distribution of Fe and Al in the surface waters of the Arabian Sea," *Deep-Sea Research Part II*, vol. 46, no. 8-9, pp. 1597–1622, 1999.

[36] J. D. Wiggert, R. G. Murtugudde, and C. R. McClain, "Processes controlling interannual variations in wintertime (Northeast Monsoon) primary productivity in the central Arabian Sea," *Deep-Sea Research Part II*, vol. 49, no. 12, pp. 2319–2343, 2002.

[37] M. R. Landry, S. L. Brown, L. Campbell, J. Constantinou, and H. Liu, "Spatial patterns in phytoplankton growth and microzooplankton grazing in the Arabian Sea during monsoon forcing," *Deep-Sea Research Part II*, vol. 45, no. 10-11, pp. 2353–2368, 1998.

[38] J. D. Wiggert, B. H. Jones, T. D. Dickey, et al., "The Northeast Monsoon's impact on mixing, phytoplankton biomass and

nutrient cycling in the Arabian Sea," *Deep-Sea Research Part II*, vol. 47, no. 7-8, pp. 1353–1385, 2000.

[39] T. Platt, S. Sathyendranath, O. Ulloa, W. G. Harrison, N. Hoepffner, and J. Goes, "Nutrient control of phytoplankton photosynthesis in the Western North Atlantic," *Nature*, vol. 356, no. 6366, pp. 229–231, 1992.

[40] S. Hastenrath and P. Lamb, *Climatic Atlas of the Indian Ocean—Part I: Surface Climate and Atmospheric Circulation*, University of Wisconsin Press, Madison, Wis, USA, 1979.

[41] K. Banse and D. C. English, "Revision of satellite-based phytoplankton pigment data from the Arabian Sea during the northeast monsoon," *Journal of Marine Research*, vol. 2, pp. 83–103, 1993.

[42] R. N. Sambrotto, H. J. Niebauer, J. J. Goering, and R. L. Iverson, "Relationships among vertical mixing, nitrate uptake, and phytoplankton growth during the spring bloom in the southeast Bering Sea middle shelf," *Continental Shelf Research*, vol. 5, no. 1-2, pp. 161–198, 1986.